Critical loss radius in a Penning trap subject to multipole fields

J. Fajans,[1,a] N. Madsen,[2] and F. Robicheaux[3]
[1]*Department of Physics, University of California at Berkeley and the Lawrence Berkeley National Laboratory, Berkeley, California 94720, USA*
[2]*Department of Physics, Swansea University, Swansea SA2 8PP, United Kingdom*
[3]*Department of Physics, Auburn University, Auburn, Alabama 36849-5311, USA*

(Received 17 December 2007; accepted 28 February 2008; published online 31 March 2008)

When particles in a Penning trap are subject to a magnetic multipole field, those beyond a critical radius will be lost. The critical radius depends on the history by which the field is applied, and can be much smaller if the particles are injected into a preexisting multipole than if the particles are subject to a ramped multipole. Both cases are relevant to ongoing experiments designed to trap antihydrogen. © *2008 American Institute of Physics*. [DOI: 10.1063/1.2899306]

I. INTRODUCTION

Two collaborations, ALPHA[1] and ATRAP,[2] are attempting to trap antihydrogen ($\bar{H}$) at CERN. The experiments are broadly similar; both use adjacent Penning traps to confine the $\bar{H}$ constituents, positrons (e^+), and antiprotons ($\bar{p}$). The Penning traps use strong solenoidal axial magnetic fields, $B_z\hat{z}$, to confine the constituents radially, and electrostatic wells to confine the constituents axially. Penning traps have been used for many years, and the behavior of particles in these traps is relatively well understood. Particles can survive for hours, sometimes days, in these traps; long confinement times are guaranteed by the azimuthal symmetry of the traps.[3]

Unlike the $\bar{H}$ constituents, $\bar{H}$ itself is uncharged; consequently, it is not confined by Penning trap fields. To trap $\bar{H}$, both collaborations intend to take advantage of $\bar{H}$'s permanent magnetic moment, which can be used to confine the $\bar{H}$ in a magnetic minimum. By superimposing a minimum-B field over the Penning trap, the collaborations hope to simultaneous hold and mix e^+ and $\bar{p}$, and create and trap $\bar{H}$. Detailed descriptions of the experiments can be found elsewhere.[2,4]

The minimum-B fields can cause particle loss. In this paper, we describe criteria that determine when such loss occurs. We use single-particle models in this paper. Such single-particle models accurately describe the motion of $\bar{p}$'s in many of the experiments performed to date. For example, in the companion paper,[5] the $\bar{p}$ energies are on the order of several eV, while the self-electrostatic potentials are on the order of mV. Thus, the $\bar{p}$ orbits in Ref. 5 are unaffected by collective effects and the single-particle model is appropriate; the $\bar{p}$ densities would have to increase by three orders of magnitude for collective effects to matter. For e^+'s, which are typically much denser in the experiments, and for mixed $e^+-\bar{p}$ plasmas, self-consistent fields may play a significant role. Nonetheless, fully self-consistent particle-in-cell (PIC) simulations[6] of dense $\bar{p}$ plasmas agree with the analytic single-particle models described here. An analytic fully self-consistent description of dense non-neutral plasmas in a strong magnetic multipole field is not yet available.

II. FIELD STRUCTURE

The minimum-B fields are created by axial magnetic mirrors added to the trap ends and a radial magnetic multipole added to the trap center. Unfortunately, the multipole fields break the azimuthal symmetry. Long e^+ and $\bar{p}$ trapping times are no longer guaranteed. Whether the Penning traps will still function adequately with these extra fields has been controversial.[6–15] Three types of multipole fields have been proposed: Quadrupole fields[16,17] such that the field at the center of the trap (ignoring the mirrors at the ends) is given, in cylindrical coordinates (r,θ,z), by

$$\mathbf{B} = B_z\hat{z} + B_w\frac{r}{R_w}[\hat{r}\cos(2\theta) - \hat{\theta}\sin(2\theta)], \tag{1}$$

sextupole fields,[15] which will not be further discussed in this paper, and octupole fields[4,18] given by

$$\mathbf{B} = B_z\hat{z} + B_w\left(\frac{r}{R_w}\right)^3[\hat{r}\cos(4\theta) - \hat{\theta}\sin(4\theta)]. \tag{2}$$

Here B_w is the multipole field at the trap wall radius R_w. As the multipole field adds quadratically to the axial field, B_w must be comparable to B_z to generate a significant minimum. Note that particles that hit the wall at R_w are lost.

Under many circumstances, the $\bar{H}$ constituents, the $\bar{p}$'s and e^+'s, closely follow field lines. Consequently, it is helpful to visualize the shape of the field lines. For the quadrupole, the field lines originating from a circular locus of points in the plane transverse to $\hat{z}$ form a twisted bowtie (see Fig. 1).[9] By definition, the bowtie is circular in the center, arbitrarily located at $z=0$, and it becomes ever more elliptical away from the center. The major axes of the ellipses are oriented along the $\hat{x}$ axis for positive z, and along $\hat{y}$ for negative z. The shape formed by the octupole is similar, with the elliptical ends being replaced by four-fluted cylinders. The flutes at one end are now rotated by 45° relative to the other end, rather than 90° as is the case for quadrupoles.

[a]Electronic mail: joel@physics.berkeley.edu. URL: socrates.berkeley.edu/~fajans.

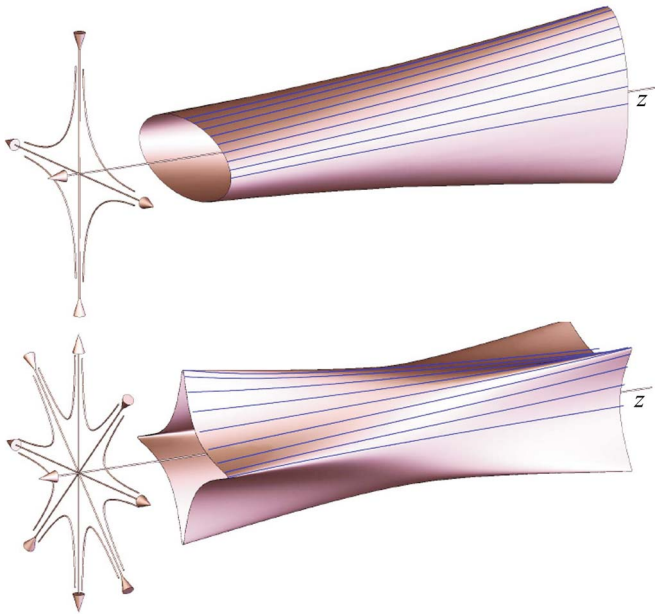

FIG. 1. (Color online) Magnetic field lines for a transverse quadrupole (top) and octupole (bottom), superimposed on a uniform axial field. For each configuration, the vectors on the left represent the directions of the axially invariant multipole and axial field components. The surface is created by following the field lines from a centered circular locus, and the lines shown within the surfaces are field lines.

So long as we use a pure axial plus transverse multipole field, the field is independent of z. Then $\nabla_\perp \cdot \mathbf{B}=0$, where $\nabla_\perp$ is the differential operator in the plane perpendicular to $\hat{z}$. Thus, the area enclosed by a set of field lines penetrating a plane perpendicular to $\hat{z}$ is independent of z; the cross-sectional area of the surfaces in Fig. 1 is invariant. Note that the mirror fields required to trap the $\bar{\mathrm{H}}$ axially break this invariance. For the ALPHA experiment, however, the mirror coils are sufficiently axially distant that the cross-sectional area is approximately invariant.

III. CHARGED PARTICLE LOSS

Particles confined by the electrostatic well within the multipole bounce back and forth while following the magnetic field lines. If any of the field lines extend to the trap wall within the length set by the electrostatic well, the particles will follow them there and be lost. This "ballistic" loss was first identified with electrons in a quadrupole magnet.[13] There exists a critical radius, r_c, which characterizes the ballistic loss process; particles that are initially beyond the critical radius are lost ballistically, while particles that are within the critical radius are not lost immediately. (The critical radius can be, but is not always, a function of the azimuthal angle θ. See the discussion later in the paper.) Particles within the critical radius will eventually be lost by diffusion. Diffusive loss occurs in the absence of multipole fields, but the multipole fields will increase the diffusion coefficient.[9] They will also decrease the radius to which the particles have to diffuse before they are lost from R_w to r_c. The net effect will be enhanced diffusive loss.

Thus, the critical radius characterizes the loss processes. The path taken by a field line is a function of its initial azimuthal angle, and is complicated by the field lines' propagation in θ as well as r. However, the fastest outward going field lines remain at the same angle, and it is easy to calculate their path. For a quadrupole, these field lines are at $\theta=0,\ \pi$ and propagate like[13]

$$r(z) = r_0 \exp\left(\frac{B_w}{B_z}\frac{z}{R_w}\right), \tag{3}$$

while for an octupole they are at $\theta=0,\ \pi/2,\ \pi$, and $3\pi/4$ and propagate outward like

$$r(z) = \frac{r_0}{\sqrt{1-2\dfrac{B_w}{B_z}\dfrac{r_0^2}{R_w^2}\dfrac{z}{R_w}}}, \tag{4}$$

where r_0 is the initial radius at $z=0$. By inverting these equations, we can find the critical radius r_c from the condition $R_w=r(z=L_{\mathrm{eff}};r_0=r_c)$, where L_{eff} is the effective length of the trap. These equations define the fastest outward propagating field lines, which occur only at the specific angles. Field lines that originate at other angles do not propagate outward as fast; indeed, some field lines propagate inward. This has a qualitatively small effect in a quadrupole as the other field lines converge toward the fastest outward propagating field lines. As can be seen in Fig. 2(a), the majority of field lines propagate outward nearly as much as the maximally outward propagating field lines. In an octupole, Fig. 2(b), this effect is less pronounced. For strong enough octupole fields, the outward transport peaks are cusp-like. Even in an octupole, however, the critical radius defined by the maximally outward propagating field lines is a good parameter for characterizing the loss. Particles that are not initially on these field lines will quickly find themselves rotated to them by the $\mathbf{E}\times\mathbf{B}$ drifts caused by the radial electrostatic fields at the trap ends and the self-electric fields, if any, in the interior of the trap.

The critical radius depends on the effective trap length L_{eff}. Two cases are common in typical experiments. In the first case, particles are held in a fixed region of the trap while the multipole field is ramped on. Previously, we used PIC simulations[6] to show that, in this case, the effective trap length, L_{eff}, is half the end-to-end bounce length L of the particles in the trap.[14] Here we show that this result is a consequence of constraints imposed by adiabatic invariants. In the second case, particles held in a short trap are injected into a longer trap, with a preexisting multipole field. This procedure has been used to mix $\bar{\mathrm{p}}$'s with e^+'s.[19] Here, the effective trap length L_{eff} can approach the full length of the trap L, and we explore the consequences of such expansions.

IV. RAMPING MULTIPOLE

In the absence of the multipole fields, particles stay at a fixed radius, say r_{00}, and bounce end-to-end while slowly orbiting the trap axis. An individual particle will cover the surface of a cylindrical shell. As the multipole is turned on this surface will deform, but is subject to certain constraints.

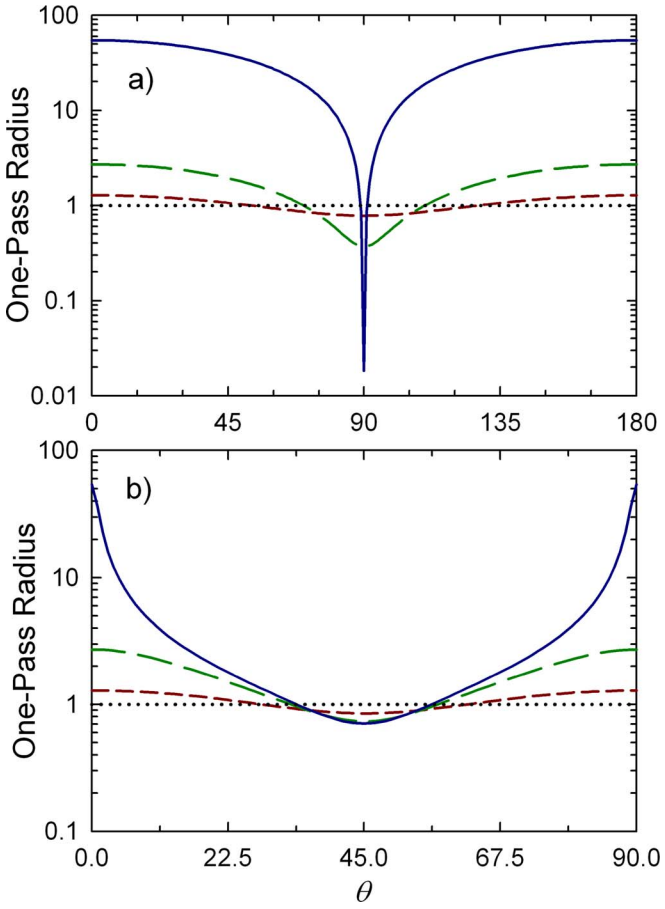

FIG. 2. (Color online) The radius after one pass across the trap as a function of initial angle θ for (a) a quadrupole and (b) an octupole. In (a), $B_w z/B_z R_w=4$ (solid), 1 (long dash), and 0.25 (short dash). The radius is normalized to the initial radius. In (b), the values of B_w are adjusted so that the maximum expansion is the same as in case (a), namely $B_w r_0^2 z/B_z R_w^3 = 0.49983$, 0.4322, and 0.197. (Note that the first value is very close to the critical value of 0.5 at which the solution is not analytic.) For strong quadrupoles, the one-pass radius is substantially less than the initial radius for only a small fraction of the initial angles.

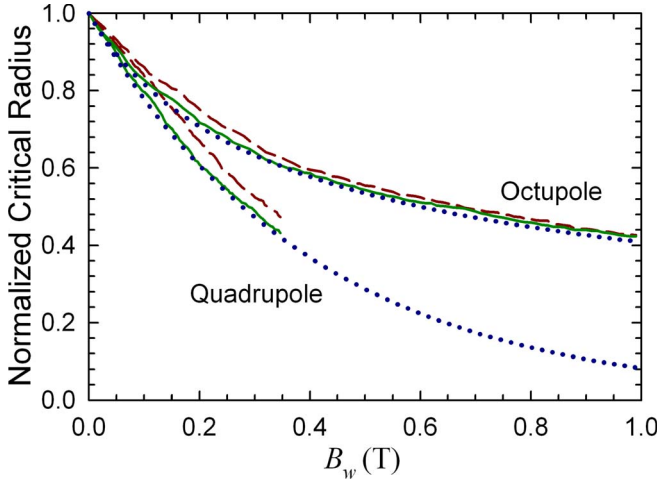

FIG. 3. (Color online) Critical radius as a function of the multipole field at the wall B_w for a ramping multipole field. Particle simulation results are shown by the lines, and the results of inverting Eqs. (5) and (6) are shown by the dots. In the simulation, the critical radius was determined by uniformly filling the trap with particles and ramping the multipole field. The normalized critical radius is the square root of the fraction of particles that have not hit the trap wall. The solid simulation lines include the effect of rotations; the dashed lines do not. The critical radius is normalized by the wall radius, $L/R_w=5$ and $B_z=1$ T.

(Here, we assume that the particles are bouncing quickly relative to their rotation time around the trap.) First, symmetry requires that surfaces at equal, but opposite, distances from the trap center be identical when rotated through the symmetry of the multipole: 90° for a quadrupole and 45° for an octupole. Further, symmetry requires that the center cross section retain the complete symmetry of the multipole. A circular cross section, of course, retains this symmetry, but simulations show that rotations around the trap axis deform the cross section into a curve with fourfold symmetry (squarish) for a quadrupole, and eightfold symmetry for an octupole.[6] Finally, as the particles drift around the central axis, their orbit's intersections with the central transverse plane (Poincaré map) trace a closed curve. This curve encloses a cross-sectional area. The magnetic flux Φ through this cross section comes solely from the time-invariant axial field; the multipole field does not contribute to Φ as it is tangential to the transverse plane. The third adiabatic invariant of plasma physics[20] requires that Φ be conserved if the octupole is ramped on slowly compared to the end-to-end bounce time. (Experimental constraints ensure that this condition is easily met.) Thus, the area of the central cross section (indeed any cross section) is invariant as the multipole field is ramped, and remains equal to the area of the initial cross section.

If the central cross section remained exactly circular, then the particles' radii at $z=0$ would remain fixed at their initial radius r_{00}. Particles would be lost if they hit the wall when traversing the half-length of the trap when starting at r_{00}. Thus, the critical radius r_c can be found from Eqs. (3) and (4) by using an effective length L_{eff} equal to half the trap length $L/2$,[14]

$$r_c = R_w \exp\left(-\frac{1}{2}\frac{B_w}{B_z}\frac{L}{R_w}\right) \tag{5}$$

for a quadrupole and

$$r_c = \frac{R_w}{\sqrt{1+\dfrac{B_w}{B_z}\dfrac{L}{R_w}}} \tag{6}$$

for an octupole.

The earlier PIC simulations[6] showed that the center cross section does not deform very much, and that L_{eff} equals $L/2$ to a very good approximation. We reproduce this result with single-particle simulations in Fig. 3. Note that the rotations make the critical radius sharp; virtually all particles beyond the critical radius are lost, and virtually all particles within the critical radius are retained.

In the absence of any other physical effects, the conservation of area result proved above requires the density to be invariant with z. If the density is initially uniform over a solid cylinder, it will remain uniform. (The density of a cold plasma in thermal equilibrium held in a pure axial field will

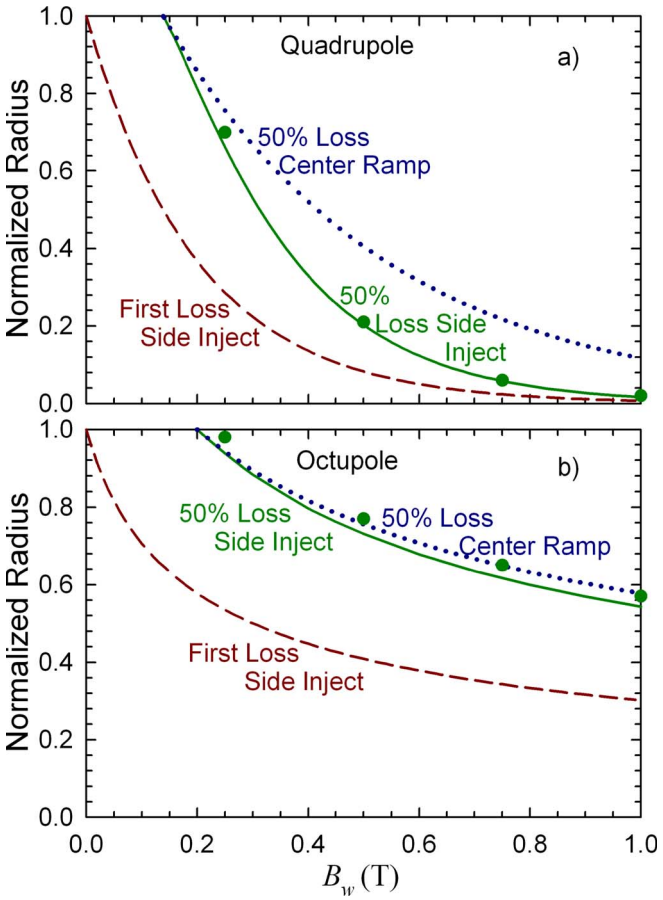

FIG. 4. (Color online) Critical radius as a function of the multipole field at the wall B_w for injection into a preexisting (a) quadrupole and (b) octupole field. For each multipole, the figures show the radius at which particles are first lost, r_{c0}, and the radius at which 50% of the particles are lost, $r_{50\%}$. [The calculated $r_{50\%}$, found via Eq. (7), was checked at the four green points shown in each graph by mulitple-bounce particle simulations.] For comparison, the figures also show the radius at which 50% of the particles would be lost for a ramped multipole. The critical radius is normalized by the wall radius, $L/R_w=5$ and $B_z=1$ T.

be uniform except near the plasma edge.[21]) However, there are at least two effects that will vary the density. First, in the presence of a multipole field, the electrostatic potential along the magnetic field lines will not be constant. (It is constant inside the plasma in a pure axial field.) If there is some collisional mechanism, the particle will distribute themselves along individual field lines according to the Boltzmann relation. Even in the absence of collisions, adiabatic trapping will force the particles to distribute themselves in a quasi-Boltzmann fashion.[22] In either case, particles will be denser at the end of the field line to which they are attracted. Second, mirroring effects will repel particles from higher magnetic field regions. If the particles are dense enough for their self-electric fields to be important, the effects of mirroring are complicated and not yet understood for multipolar fields.[23–25]

Note that the simulations presented here include the effects of the electrostatic background field. We used a fairly sharp, hard-wall potential to tightly control the orbit length. The simulation generally used the guiding center approximation, but was checked by comparison to the full equations of motion. Thus, mirroring and $\mathbf{E}\times\mathbf{B}$ drifts were included. The simulation does not include effects due to collisions or to the self-electric field of the particles. In the experiments, the $\bar{p}$ self-electric fields are generally small and can be safely neglected. The e^+ fields are not small, and could affect the results presented here. However, earlier PIC simulations,[6] which include the self-electric fields, found very similar critical radii.

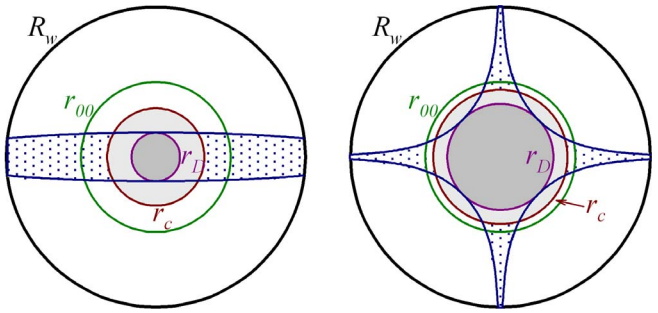

FIG. 5. (Color online) End view of the relevant surfaces for side injection into a preexisting quadruple (left) and octupole (right). Before injection, particles are held contained on one side inside a circle of radius r_{00}. On their first pass through $z=0$ after release, the particles are confined within the ellipse (quadrupole) or fluted cylinder (octupole) with cutoff tips. Only particles that are within the critical radius r_c will survive subsequent passes. The density of particles within r_D will remain approximately unchanged, but as the arms of the ellipse (flutes) between r_D and r_c rotate, the coarse-grained density in this latter region will decrease.

V. SIDE INJECTION INTO A PREEXISTING MULTIPOLE

There is less symmetry when particles are injected into a preexisting multipole field, and the results are more complicated. We will assume that the initial, pre-injection, trap length is sufficiently short that the particles can be taken to start uniformly distributed in a cylinder of radius r_{00} despite the already present multipole field. We further assume that the particles start at a near uniform position of $z=-L/2$. Some of the particles will follow the fastest expanding field lines all the way to $z=L/2$. Thus, the critical radius r_{c0} for the first loss associated with the initial distribution at $z=-L/2$ will be determined by the effective length $L_{\text{eff}}=L$ (see Fig. 4).

Not all particles whose radius is larger than r_{c0} will be lost, however. The surviving fraction can be found by tracing the locus of points at r_{00} from $z=-L/2$ to $z=0$ (see Fig. 5). Some particles will have moved in, and some will have moved out. Those particles that are beyond the critical radius r_c associated with the distribution at $z=0$, defined by Eq. (5) or Eq. (6), will be lost. The surviving fraction will be equal to the area of the curve traced by this locus that is inside the critical radius r_c, divided by the initial area. Rather than using the critical radius of first loss r_{c0} to characterize the loss process, a better measure is the radius $r_{50\%}$ of a uniformly filled cylinder which would lead to 50% loss. A cylinder of radius any greater than $r_{50\%}$ would lose more than 50% of its particles, and a cylinder of less than $r_{50\%}$ would lose less. This radius can be found by iteratively solving for the value of r_{00} that gives 50% survival, i.e., by solving

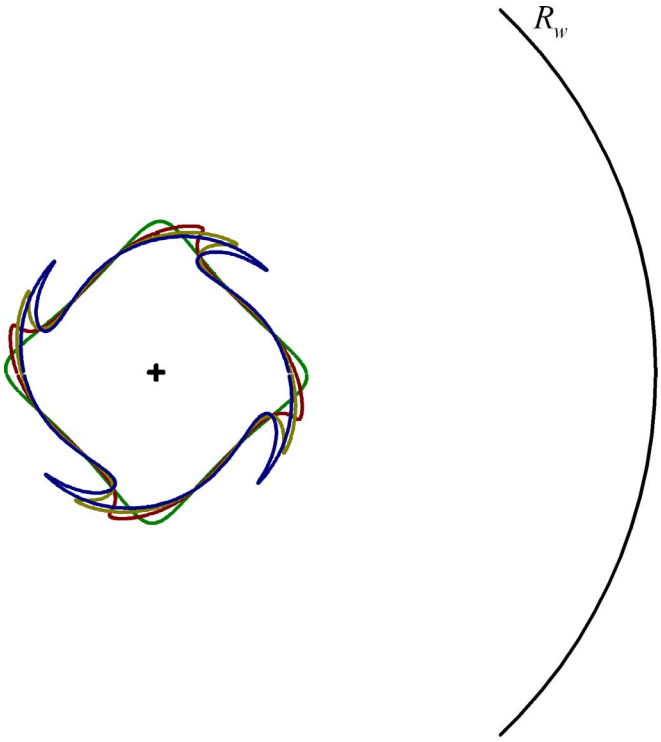

FIG. 6. (Color online) The development of density-smearing spiral arms described in the text. Particles in a circle of radius 5 mm are injected into a $B_w=1$ T octupole. The well length is 100 mm. The nearly square curve is the boundary of the plasma as it passes through $z=0$ the first time; the next three curves show the boundary after the particles have revolved around the trap axis π, 2π and 3π radians.

$$\frac{1}{2}=\frac{1}{\pi r_{50\%}^2}\int_0^{2\pi}d\theta\int_0^{\min[r(L/2;\theta),r_c]}rdr, \tag{7}$$

where $r(L/2;\theta)$ is the radius of particle that starts at position $(r_{50\%}, \theta, z=-L/2)$, and follows the field lines to $z=0$.

Figure 4 plots $r_{50\%}$, and compares it to the equivalent radius for particles confined in a ramping multipole. [For a ramping multipole, the 50% loss radius is $\sqrt{2}$ times the critical radius r_c defined by Eq. (5) or Eq. (6); all the charge within r_c will be retained, and all the charge between r_c and $\sqrt{2}r_c$ will be lost. Thus, assuming constant initial density, half the charge will be lost.]

For a quadrupole, the 50% loss side-injection critical radius approaches the first loss radius r_{c0} at high field. For an octupole, however, the 50% loss side-injection critical radius is only slightly less than the 50% loss ramping critical radius. The one-pass octupole radii cusp shown in Fig. 2 cause this difference in behavior.

With the ramped field, the density is quasi-uniform. This is not the case with side injection into a preexisting field. A new radius r_D is defined by following the fastest *inwardly* directed field line originating at r_{00} to $z=0$ (see Fig. 5). The quasicircular disk defined by r_D will start, and remain, uniformly filled at the original density (ignoring the complications described above). Between r_D and r_c, the initial density will equal the initial density at some angles and zero at others. The particles in this region will orbit the trap axis at nonuniform rates. The simple initial boundary will deform into spiral arms (see Fig. 6). Inside the arms, the density will remain at the initial density, and outside the arms the density will remain zero. As the arms elongate, course-graining will make it appear that the density is independent of angle and declining with r between r_D and r_c. Eventually, collisions will genuinely smooth the density in this region. Thus, the density profile will be uniform out to r_D, smoothly diminishing between r_D and r_c, and zero beyond r_c. Transport across field lines toward a final global equilibrium state will further evolve the distribution.

VI. CONCLUSIONS

We have explored the difference between two different methods of subjecting particles in a Penning trap to a magnetic multipole field. Both methods are relevant to trapping antihydrogen produced by standard mixing schemes.[19,26] Fewer particles are lost when the particles are subject to a ramping field than when the particles are injected into a preexisting quadrupole field, but the loss is almost identical for an octupole. In the absence of complicating effects, the density of the remaining particles is uniform (assuming the initial density is uniform) in the first case, but not in the second.

The results presented here do not take into account the fields from the magnetic mirrors also present in the experiments. For ALPHA,[4] the mirror coils are far enough away that the fields do not significantly change the results.

We have also assumed that the particles bounce quickly compared to their axial rotation period. This is a good assumption for hot e^+'s and $\bar{p}$'s, but it is not necessarily satisfied for particles that have cooled to 4.2 K. If it is not satisfied, the resonant effects described in Ref. 9 may become important.

ACKNOWLEDGMENTS

We thank our colleagues in the ALPHA collaboration for their helpful comments.

This work was supported by the Department of Energy (USA) and EPSRC and the Leverhulme Trust (UK).

[1] G. Andresen, W. Bertsche, A. Boston, P. D. Bowe, C. L. Cesar, S. Chapman, M. Charlton, M. Chartier, A. Deutsch, J. Fajans, M. C. Fujiwara, R. Funakoshi, D. R. Gill, K. Gomberoff, J. S. Hangst, R. S. Hayano, R. Hydomako, M. J. Jenkins, L. V. Jørgensen, L. Kurchaninov, N. Madsen, P. Nolan, K. Olchanski, A. Olin, A. Povilus, F. Robicheaux, E. Sarid, D. M. Silveira, J. W. Storey, H. H. Telle, R. I. Thompson, D. P. van der Werf, J. S. Wurtele, and Y. Yamazaki, Phys. Rev. Lett. **98**, 023402 (2007).

[2] G. Gabrielse, P. Larochelle, D. L. Sage, B. Levitt, W. S. Kolthammer, I. Kuljanishvili, R. McConnell, J. Wrubel, F. M. Esser, H. Glückler, D. Grzonka, G. Hansen, S. Martin, W. Oelert, J. Schillings, M. Schmitt, T. Sefzick, H. Soltner, Z. Zhang, D. Comeau, M. C. George, E. A. Hessels, C. H. Storry, M. Weel, A. Speck, F. Nillius, J. Walz, and T. W. Hänsch, Phys. Rev. Lett. **98**, 113002 (2007).

[3] T. M. O'Neil, Phys. Fluids **23**, 2216 (1980).

[4] W. Bertsche, A. Boston, P. Bowe, C. Cesar, S. Chapman, M. Charlton, M. Chartier, A. Deutsch, J. Fajans, M. Fujiwara, R. Funakoshi, K. Gomberoff, J. Hangst, R. Hayano, M. J. Jenkins, L. V. Jørgensen, P. Ko, N. Madsen, P. Nolan, R. Page, L. Posada, A. Povilus, E. Sarid, D. M. Silveira, D. van der Werf, Y. Yamazaki, B. Parker, J. Escallier, and A. Ghosh, Nucl. Instrum. Methods Phys. Res. A **566**, 746 (2006).

[5] G. Andresen, W. Bertsche, P. D. Bowe, C. C. Bray, E. Butler, C. L. Cesar, S. Chapman, M. Charlton, J. Fajans, M. C. Fujiwara, R. Funakoshi, D. R. Gill, J. S. Hangst, W. N. Hardy, R. S. Hayano, M. E. Hayden, A. J. Humphries, R. Hydomako, M. J. Jenkins, L. V. Jørgensen, L. Kurchani-

nov, R. Lambo, N. Madsen, P. Nolan, K. Olchanski, A. Olin, R. D. Page, A. Povilus, P. Pusa, F. Robicheaux, E. Sarid, S. S. E. Nasr, D. M. Silveira, J. W. Storey, R. I. Thompson, D. P. van der Werf, J. S. Wurtele, and Y. Yamazaki, Phys. Plasmas **15**, 032107 (2008).
[6]K. Gomberoff, J. Fajans, A. Friedman, D. P. Grote, R. H. Cohen, J.-L. Vay, and J. Wurtele, Phys. Plasmas **14**, 102111 (2007).
[7]E. Gilson and J. Fajans, AIP Conf. Proc. **498**, 250 (1999).
[8]T. Squires, P. Yesley, and G. Gabrielse, Phys. Rev. Lett. **86**, 5266 (2001).
[9]E. Gilson and J. Fajans, Phys. Rev. Lett. **90**, 015001 (2003).
[10]M. Holzscheiter, M. Charlton, and M. Nieto, Phys. Rep. **402**, 1 (2004).
[11]G. Gabrielse, Adv. At., Mol., Opt. Phys. **50**, 155 (2005).
[12]A. J. Speck, Ph.D. thesis, Harvard University (2005).
[13]J. Fajans, W. Bertsche, K. Burke, S. F. Chapman, and D. P. van der Werf, Phys. Rev. Lett. **95**, 155001 (2005).
[14]J. Fajans, W. Bertsche, K. Burke, A. Deutsch, S. F. Chapman, K. Gomberoff, D. P. van der Werf, and J. S. Wurtele, AIP Conf. Proc. **862**, 176 (2006).
[15]M. Amoretti, C. Canali, C. Carrare, M. Doser, V. Lagomarsino, G. Manuzio, G. Testera, and S. Zavatarelli, Phys. Lett. A **360**, 141 (2006).
[16]B. Deutch, F. Jacobsen, L. Andersen, P. Hvelplund, H. Knudsen, M. Holzscheiter, M. Charlton, and G. Laricchia, Phys. Scr., T **T22**, 248 (1988).
[17]G. Gabrielse, L. Haarsma, S. Rolston, and W. Kells, Phys. Lett. A **129**, 38 (1988).
[18]J. Fajans and A. Schmidt, Nucl. Instrum. Methods Phys. Res. A **521**, 318 (2004).
[19]M. Amoretti, C. Amsler, G. Bonomi, A. Bouchta, P. Bowe, C. Carraro, C. Cesar, M. Charlton, M. J. T. Collier, M. Doser, V. Filippini, K. S. Fine, A. Fontana, M. C. Fujiwara, R. Funakoshi, P. Genova, J. S. Hangst, R. S. Hayano, M. H. Holzscheiter, L. V. Jørgensen, V. Lagomarsino, R. Landua, D. Lindelöf, E. Lodi-Rizzini, M. Macrì, N. Madsen, G. Manuzio, M. Marchesotti, P. Montagna, H. Pruys, C. Regenfus, P. Riedler, J. Rochet, A. Rotondi, G. Rouleau, G. Testera, A. Variola, T. L. Watson, and D. P. van der Werf, Nature (London) **419**, 456 (2002).
[20]F. Chen, *Introduction to Plasma Physics and Controlled Fusion* (Springer, New York, 1984).
[21]T. M. O'Neil and C. F. Driscoll, Phys. Fluids **22**, 266 (1979).
[22]C. Hansen and J. Fajans, Phys. Rev. Lett. **74**, 4209 (1995).
[23]J. Fajans, Phys. Plasmas **10**, 1209 (2003).
[24]I. A. Kotelnikov, M. Rome, and A. Kabantsev, Phys. Plasmas **13**, 092108 (2006).
[25]K. Gomberoff, J. Fajans, J. Wurtele, A. Friedman, D. P. Grote, R. H. Cohen, and J.-L. Vay, Phys. Plasmas **14**, 052107 (2007).
[26]G. Gabrielse, N. S. Bowden, P. Oxley, A. Speck, C. H. Storry, J. N. Tan, M. Wessels, D. Grzonka, W. Oelert, G. Schepers, T. Sefzick, J. Walz, H. Pittner, T. W. Hänsch, and E. A. Hessels, Phys. Rev. Lett. **89**, 213401 (2002).